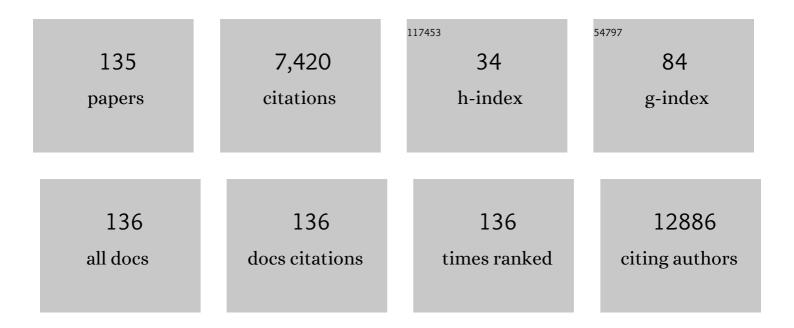
List of Publications by Year in descending order

Source: https://exaly.com/author-pdf/7433573/publications.pdf Version: 2024-02-01



#	Article	IF	CITATIONS
1	3D Porous Graphene Films with Largeâ€Area Inâ€Plane Exterior Skins. Advanced Materials Interfaces, 2022, 9, .	1.9	3
2	A Flexible and Ultraâ€Wideband Terahertz Wave Absorber Based on Pyramidâ€Shaped Carbon Nanotube Array via Femtosecond‣aser Microprocessing and Twoâ€Step Transfer Technique. Advanced Materials Interfaces, 2022, 9, .	1.9	5
3	Electrostatic Coupling in MoS ₂ /CuInP ₂ S ₆ Ferroelectric vdW Heterostructures. Advanced Functional Materials, 2022, 32, .	7.8	17
4	Thermally Conductive and Leakage-Proof Phase-Change Materials Composed of Dense Graphene Foam and Paraffin for Thermal Management. ACS Applied Nano Materials, 2022, 5, 8362-8370.	2.4	10
5	Programmable morphing, electroactive porous shape memory polymer composites with battery-voltage Joule heating stimulated recovery. APL Materials, 2022, 10, 071109.	2.2	2
6	An effective thermal conductivity model for architected phase change material enhancer: Theoretical and experimental investigations. International Journal of Heat and Mass Transfer, 2021, 176, 121364.	2.5	11
7	Boron nanosheets induced microstructure and charge transfer tailoring in carbon nanofibrous mats towards highly efficient water splitting. Nano Energy, 2021, 88, 106246.	8.2	15
8	Effect of loading fraction of three-dimensional graphene foam (3D-C) on thermal, mechanical, and shape memory properties of 3D-C/SMP composite. Materials Research Bulletin, 2021, 142, 111378.	2.7	9
9	Lightweight, Superelastic Boron Nitride/Polydimethylsiloxane Foam as Air Dielectric Substitute for Multifunctional Capacitive Sensor Applications. Advanced Functional Materials, 2020, 30, 1909604.	7.8	117
10	Experimental characterization of three-dimensional Graphene's thermoacoustic response and its theoretical modelling. Carbon, 2020, 169, 382-394.	5.4	6
11	Imaging the defect distribution in 2D hexagonal boron nitride by tracing photogenerated electron dynamics. Journal Physics D: Applied Physics, 2020, 53, 405106.	1.3	5
12	Dielectric dispersion and superior thermal characteristics in isotope-enriched hexagonal boron nitride thin films: evaluation as thermally self-dissipating dielectrics for GaN transistors. Journal of Materials Chemistry C, 2020, 8, 9558-9568.	2.7	4
13	One-dimensional hexagonal boron nitride conducting channel. Science Advances, 2020, 6, eaay4958.	4.7	37
14	Nitrogen-mediated aligned growth of hexagonal BN films for reliable high-performance InSe transistors. Journal of Materials Chemistry C, 2020, 8, 4421-4431.	2.7	5
15	Versatile and scalable chemical vapor deposition of vertically aligned MoTe2 on reusable Mo foils. Nano Research, 2020, 13, 2371-2377.	5.8	5
16	On the recovery of 2DEG properties in vertically ordered h-BN deposited AlGaN/GaN heterostructures on Si substrate. Applied Physics Express, 2020, 13, 065508.	1.1	7
17	Synthesis of Atomically Thin 1Tâ€TaSe ₂ with a Strongly Enhanced Chargeâ€Densityâ€Wave Order. Advanced Functional Materials, 2020, 30, 2001903.	7.8	15
18	POSS enhanced 3D graphene - Polyimide film for atomic oxygen endurance in Low Earth Orbit space environment. Polymer, 2020, 191, 122270.	1.8	37

EDWIN HANG TONG TEO

#	Article	IF	CITATIONS
19	A flexible and ultra-broadband terahertz wave absorber based on graphene–vertically aligned carbon nanotube hybrids. Journal of Materials Chemistry C, 2020, 8, 7244-7252.	2.7	16
20	Wafer-scale vertically aligned carbon nanotubes for broadband terahertz wave absorption. Carbon, 2019, 154, 503-509.	5.4	20
21	Manipulating Coherent Light–Matter Interaction: Continuous Transition between Strong Coupling and Weak Coupling in MoS ₂ Monolayer Coupled with Plasmonic Nanocavities. Advanced Optical Materials, 2019, 7, 1900857.	3.6	48
22	Phonon Polaritons in Monolayers of Hexagonal Boron Nitride. Advanced Materials, 2019, 31, e1806603.	11.1	73
23	A corner reflector of graphene Dirac fermions as a phonon-scattering sensor. Nature Communications, 2019, 10, 2428.	5.8	7
24	Flexible Ultra-Wideband Terahertz Absorber Based on Vertically Aligned Carbon Nanotubes. ACS Applied Materials & Interfaces, 2019, 11, 43671-43680.	4.0	39
25	Boron Nitride Coated Three-Dimensional Graphene as an Electrically Insulating Electromagnetic Interference Shield. , 2019, , .		2
26	Elastic Properties of 2D Ultrathin Tungsten Nitride Crystals Grown by Chemical Vapor Deposition. Advanced Functional Materials, 2019, 29, 1902663.	7.8	37
27	Double-Spiral Hexagonal Boron Nitride and Shear Strained Coalescence Boundary. Nano Letters, 2019, 19, 4229-4236.	4.5	15
28	Concurrent Inhibition and Redistribution of Spontaneous Emission from All Inorganic Perovskite Photonic Crystals. ACS Photonics, 2019, 6, 1331-1337.	3.2	39
29	Guest Editorial Special Section on the Second Electron Devices Technology and Manufacturing (EDTM) Conference 2019. IEEE Journal of the Electron Devices Society, 2019, 7, 1200-1200.	1.2	0
30	Supercompressible Coaxial Carbon Nanotube@Graphene Arrays with Invariant Viscoelasticity over â~'100 to 500 °C in Ambient Air. ACS Applied Materials & Interfaces, 2018, 10, 9688-9695.	4.0	10
31	Human Rett-derived neuronal progenitor cells in 3D graphene scaffold as an <i>in vitro</i> platform to study the effect of electrical stimulation on neuronal differentiation. Biomedical Materials (Bristol), 2018, 13, 034111.	1.7	32
32	A thermal study of amorphous and textured carbon and carbon nitride thin films via transient grating spectroscopy. Carbon, 2018, 130, 355-361.	5.4	6
33	Scalable Production of Few-Layer Boron Sheets by Liquid-Phase Exfoliation and Their Superior Supercapacitive Performance. ACS Nano, 2018, 12, 1262-1272.	7.3	177
34	Largeâ€Area Atomic Layers of the Chargeâ€Densityâ€Wave Conductor TiSe ₂ . Advanced Materials, 2018, 30, 1704382.	11.1	60
35	Reliability Studies of a Super-Durable 3-D-Foam-Based TIM for All Environments. IEEE Transactions on Device and Materials Reliability, 2018, 18, 273-278.	1.5	1
36	Flexible thermal rectifier based on macroscopic PDMS@graphite composite film with asymmetric cone-shape interfaces. Carbon, 2018, 126, 464-471.	5.4	11

EDWIN HANG TONG TEO

#	Article	IF	CITATIONS
37	Localized emission from laser-irradiated defects in 2D hexagonal boron nitride. 2D Materials, 2018, 5, 015010.	2.0	65
38	Strong electro-optically active Ni-substituted Pb(Zr _{0.35} Ti _{0.65})O ₃ thin films: toward integrated active and durable photonic devices. Journal of Materials Chemistry C, 2018, 6, 12919-12927.	2.7	9
39	Engineering of High-Density Thin-Layer Graphite Foam-Based Composite Architectures with Superior Compressibility and Excellent Electromagnetic Interference Shielding Performance. ACS Applied Materials & Interfaces, 2018, 10, 41707-41716.	4.0	55
40	Gate voltage and temperature dependent Ti-graphene junction resistance toward straightforward p-n junction formation. Journal of Applied Physics, 2018, 124, .	1.1	8
41	Waferâ€Scale Vertically Aligned Carbon Nanotubes Locked by In Situ Hydrogelation toward Strengthening Static and Dynamic Compressive Responses. Macromolecular Materials and Engineering, 2018, 303, 1800024.	1.7	6
42	Landau Velocity for Collective Quantum Hall Breakdown in Bilayer Graphene. Physical Review Letters, 2018, 121, 136804.	2.9	6
43	Ultra-long wavelength Dirac plasmons in graphene capacitors. JPhys Materials, 2018, 1, 01LT02.	1.8	17
44	Concentric and Spiral Few-Layer Graphene: Growth Driven by Interfacial Nucleation vs Screw Dislocation. Chemistry of Materials, 2018, 30, 6858-6866.	3.2	21
45	Light emission from localised point defects induced in GaN crystal by a femtosecond-pulsed laser. Optical Materials Express, 2018, 8, 2703.	1.6	17
46	Concentric dopant segregation in CVD-grown N-doped graphene single crystals. Applied Surface Science, 2018, 454, 121-129.	3.1	5
47	Smoothening of wrinkles in CVD-grown hexagonal boron nitride films. Nanoscale, 2018, 10, 16243-16251.	2.8	15
48	Novel timed and self-resistive heating shape memory polymer hybrid for large area and energy efficient application. Carbon, 2018, 139, 626-634.	5.4	15
49	Anisotropic thermal conductivity of vertically self-ordered Nanocrystalline Boron Nitride thin films for thermal hotspot mitigation in electronics. , 2018, , .		0
50	EXPERIMENTAL INVESTIGATION ON HIGH HEAT FLUX SPRAY COOLING USING WATER ON COATED AND STRUCTURED SURFACES. , 2018, , .		0
51	Direct Observation of Indium Conductive Filaments in Transparent, Flexible, and Transferable Resistive Switching Memory. ACS Nano, 2017, 11, 1712-1718.	7.3	83
52	High-Density 3D-Boron Nitride and 3D-Graphene for High-Performance Nano–Thermal Interface Material. ACS Nano, 2017, 11, 2033-2044.	7.3	152
53	Control of Nanoplane Orientation in voBN for High Thermal Anisotropy in a Dielectric Thin Film: A New Solution for Thermal Hotspot Mitigation in Electronics. ACS Applied Materials & Interfaces, 2017, 9, 7456-7464.	4.0	9
54	Thermal Conductivity Enhancement of Coaxial Carbon@Boron Nitride Nanotube Arrays. ACS Applied Materials & Interfaces, 2017, 9, 14555-14560.	4.0	35

#	Article	IF	CITATIONS
55	Biocompatible Hydroxylated Boron Nitride Nanosheets/Poly(vinyl alcohol) Interpenetrating Hydrogels with Enhanced Mechanical and Thermal Responses. ACS Nano, 2017, 11, 3742-3751.	7.3	191
56	Composition-controlled synthesis and tunable optical properties of ternary boron carbonitride nanotubes. RSC Advances, 2017, 7, 12511-12517.	1.7	14
57	The Electrochemical Response of Single Crystalline Copper Nanowires to Atmospheric Air and Aqueous Solution. Small, 2017, 13, 1603411.	5.2	15
58	High-quality monolayer superconductor NbSe2 grown by chemical vapour deposition. Nature Communications, 2017, 8, 394.	5.8	290
59	A "hairy―polymer/3D-foam hybrid for flexible high performance thermal gap filling applications in harsh environments. RSC Advances, 2017, 7, 39292-39298.	1.7	2
60	Multifunctional and highly compressive cross-linker-free sponge based on reduced graphene oxide and boron nitride nanosheets. Chemical Engineering Journal, 2017, 328, 825-833.	6.6	30
61	Tuning electro-optic susceptibity via strain engineering in artificial PZT multilayer films for high-performance broadband modulator. Applied Surface Science, 2017, 425, 1059-1065.	3.1	8
62	Investigation of electronic band structure and charge transfer mechanism of oxidized three-dimensional graphene as metal-free anodes material for dye sensitized solar cell application. Chemical Physics Letters, 2017, 685, 442-450.	1.2	6
63	Laser writing of localized color centers in hexagonal boron nitrides monolayers. , 2017, , .		0
64	Threeâ€Dimensional Graphene: A Biocompatible and Biodegradable Scaffold with Enhanced Oxygenation. Advanced Healthcare Materials, 2016, 5, 1177-1191.	3.9	31
65	Hexagonal Boron Nitride Thin Film for Flexible Resistive Memory Applications. Advanced Functional Materials, 2016, 26, 2176-2184.	7.8	167
66	Ferroelectric BiFeO3 thin-film optical modulators. Applied Physics Letters, 2016, 108, .	1.5	12
67	Coaxial carbon@boron nitride nanotube arrays with enhanced thermal stability and compressive mechanical properties. Nanoscale, 2016, 8, 11114-11122.	2.8	30
68	Enhancement of polyimide and 3D graphene-polyimide through thermoforming and its effect on mechanical properties and associated creep phenomenon. Polymer Degradation and Stability, 2016, 134, 237-244.	2.7	5
69	Heat Dissipation Enhancement of 2.5D Package with 3D Graphene and 3D Boron Nitride Networks as Thermal Interface Material (TIM). , 2016, , .		4
70	Microwave and Millimeter Wave Properties of Vertically-Aligned Single Wall Carbon Nanotubes Films. Journal of Electronic Materials, 2016, 45, 2433-2441.	1.0	3
71	Trimethylamine Borane: A New Single-Source Precursor for Monolayer h-BN Single Crystals and h-BCN Thin Films. Chemistry of Materials, 2016, 28, 2180-2190.	3.2	62
72	Effect of annealing temperature on physical properties of nanostructured TiN/3DG composite. Materials and Design, 2016, 90, 524-531.	3.3	5

#	Article	IF	CITATIONS
73	Low-Temperature in Situ Growth of Graphene on Metallic Substrates and Its Application in Anticorrosion. ACS Applied Materials & amp; Interfaces, 2016, 8, 502-510.	4.0	78
74	Synthesis of aligned symmetrical multifaceted monolayer hexagonal boron nitride single crystals on resolidified copper. Nanoscale, 2016, 8, 2434-2444.	2.8	81
75	Probing the Atomic Structures of Synthetic Monolayer and Bilayer Hexagonal Boron Nitride Using Electron Microscopy. Applied Microscopy, 2016, 46, 217-226.	0.8	3
76	3D Graphene-Infused Polyimide with Enhanced Electrothermal Performance for Long-Term Flexible Space Applications. Small, 2015, 11, 6425-6434.	5.2	59
77	Controllable Synthesis of Highly Luminescent Boron Nitride Quantum Dots. Small, 2015, 11, 6491-6499.	5.2	148
78	A wafer-scale graphene and ferroelectric multilayer for flexible and fast-switched modulation applications. Nanoscale, 2015, 7, 14730-14737.	2.8	26
79	Direct growth of nanocrystalline hexagonal boron nitride films on dielectric substrates. Applied Physics Letters, 2015, 106, .	1.5	60
80	Reduced Graphene Oxide/Boron Nitride Composite Film as a Novel Binder-Free Anode for Lithium Ion Batteries with Enhanced Performances. Electrochimica Acta, 2015, 166, 197-205.	2.6	69
81	Facile Synthesis of Millimeter-Scale Vertically Aligned Boron Nitride Nanotube Forests by Template-Assisted Chemical Vapor Deposition. Chemistry of Materials, 2015, 27, 7156-7163.	3.2	47
82	Vertically self-ordered orientation of nanocrystalline hexagonal boron nitride thin films for enhanced thermal characteristics. Nanoscale, 2015, 7, 18984-18991.	2.8	26
83	Effect of titanium nitride coating on physical properties of three-dimensional graphene. Applied Surface Science, 2015, 356, 399-407.	3.1	6
84	Optical and electro-optic anisotropy of epitaxial PZT thin films. Applied Physics Letters, 2015, 107, .	1.5	30
85	Surface energy controlled growth of single crystalline two-dimensional hexagonal (h)-boron nitride. , 2014, , .		Ο
86	Three-dimensional graphene based passively mode-locked fiber laser. Optics Express, 2014, 22, 31458.	1.7	11
87	Growth of Large Single-Crystalline Two-Dimensional Boron Nitride Hexagons on Electropolished Copper. Nano Letters, 2014, 14, 839-846.	4.5	275
88	Band gap effects of hexagonal boron nitride using oxygen plasma. Applied Physics Letters, 2014, 104, .	1.5	82
89	A systematic study of the atmospheric pressure growth of large-area hexagonal crystalline boron nitride film. Journal of Materials Chemistry C, 2014, 2, 1650.	2.7	72
90	Configurable Threeâ€Dimensional Boron Nitride–Carbon Architecture and Its Tunable Electronic Behavior with Stable Thermal Performances. Small, 2014, 10, 2992-2999.	5.2	50

#	Article	IF	CITATIONS
91	Foams: Configurable Three-Dimensional Boron Nitride-Carbon Architecture and Its Tunable Electronic Behavior with Stable Thermal Performances (Small 15/2014). Small, 2014, 10, 2966-2966.	5.2	1
92	Core–shell CNT–Ni–Si nanowires as a high performance anode material for lithium ion batteries. Carbon, 2013, 63, 54-60.	5.4	41
93	Formation of thick textured carbon film using filtered cathodic vacuum arc technique. , 2013, , .		0
94	The influence of titanium nitride barrier layer on the properties of CNT bundles. , 2013, , .		0
95	Identifying the mechanisms of p-to-n conversion in unipolar graphene field-effect transistors. Nanotechnology, 2013, 24, 195202.	1.3	8
96	Growth of Carbon Nanotubes on Carbon/Cobalt Films with Different sp ^{2} /sp ^{3} Ratios. Journal of Nanomaterials, 2013, 2013, 1-5.	1.5	0
97	Formation of Thick Textured Carbon Film Using Filtered Cathodic Vacuum Arc Technique. Nanoscience and Nanotechnology Letters, 2013, 5, 912-915.	0.4	0
98	Tuning the Kapitza resistance in pillared-graphene nanostructures. Journal of Applied Physics, 2012, 111,	1.1	11
99	Thermal rectification reversal in carbon nanotubes. Journal of Applied Physics, 2012, 112, .	1.1	7
100	Phononic and structural response to strain in wurtzite-gallium nitride nanowires. Journal of Applied Physics, 2012, 111, 103506.	1.1	13
101	Electrical properties of textured carbon film formed by pulsed laser annealing. Diamond and Related Materials, 2012, 23, 135-139.	1.8	11
102	Effect of initial sp3 content on bonding structure evolution of amorphous carbon upon pulsed laser annealing. Diamond and Related Materials, 2012, 30, 48-52.	1.8	16
103	Morphology-tunable assembly of periodically aligned Si nanowire and radial pn junction arrays for solar cell applications. Applied Surface Science, 2012, 258, 6169-6176.	3.1	17
104	Carbon nanotube bumps for the flip chip packaging system. Nanoscale Research Letters, 2012, 7, 105.	3.1	29
105	Thickness dependency of field emission in amorphous and nanostructured carbon thin films. Nanoscale Research Letters, 2012, 7, 286.	3.1	7
106	Carbon based multi-functional materials towards 3D system integration. Application to thermal and interconnect management. , 2012, , .		0
107	Phonon localization around vacancies in graphene nanoribbons. Diamond and Related Materials, 2012, 23, 88-92.	1.8	40
108	From Bulk to Monolayer MoS ₂ : Evolution of Raman Scattering. Advanced Functional Materials, 2012, 22, 1385-1390.	7.8	3,354

EDWIN HANG TONG TEO

#	Article	IF	CITATIONS
109	Reâ€ordering Chaotic Carbon: Origins and Application of Textured Carbon. Advanced Materials, 2012, 24, 4112-4123.	11.1	25
110	Thermal conductivity of nanocrystalline carbon films studied by pulsed photothermal reflectance. Carbon, 2012, 50, 1428-1431.	5.4	19
111	Microstructure and through-film electrical characteristics of vertically aligned amorphous carbon films. Diamond and Related Materials, 2011, 20, 290-293.	1.8	18
112	Nanostructured carbon films with oriented graphitic planes. Applied Physics Letters, 2011, 98, 123104.	1.5	10
113	Compounded effect of vacancy on interfacial thermal transport in diamond–graphene nanostructures. Diamond and Related Materials, 2011, 20, 1137-1142.	1.8	7
114	Field emission enhancement and microstructural changes of carbon films by single pulse laser irradiation. Carbon, 2011, 49, 1018-1024.	5.4	29
115	Plasma density induced formation of nanocrystals in physical vapor deposited carbon films. Carbon, 2011, 49, 1733-1744.	5.4	34
116	Nano-patterning of through-film conductivity in anisotropic amorphous carbon induced using conductive atomic force microscopy. Carbon, 2011, 49, 2679-2682.	5.4	14
117	Characterization of CNT interconnection bumps implemented for 1st level flip chip packaging. , 2011, , .		3
118	Interpillar phononics in pillared-graphene hybrid nanostructures. Journal of Applied Physics, 2011, 110, 083502.	1.1	15
119	Thermal transport around tears in graphene. Journal of Applied Physics, 2011, 109, 043508-043508-6.	1.1	3
120	Carbon metal composite film deposited using novel Filtered Cathodic Vacuum Arc technique. , 2011, , .		0
121	Impact of the CNT growth process on gold metallization dedicated to RF interconnect applications. International Journal of Microwave and Wireless Technologies, 2010, 2, 463-469.	1.5	10
122	Flux-mediated diffuse mismatch model. Applied Physics Letters, 2010, 97, .	1.5	17
123	Microstructure and electrical properties of in-situ annealed carbon films. , 2010, , .		1
124	Quantitative, nanoscale mapping of sp2 percentage and crystal orientation in carbon multilayers. Carbon, 2009, 47, 94-101.	5.4	24
125	The origin of preferred orientation during carbon film growth. Journal of Physics Condensed Matter, 2009, 21, 225003.	0.7	15
126	Superhydrophobic carbon nanotube/amorphous carbon nanosphere hybrid film. Diamond and Related Materials, 2009, 18, 1235-1238.	1.8	21

#	Article	IF	CITATIONS
127	Mechanical properties of gradient pulse biased amorphous carbon film. Thin Solid Films, 2008, 516, 5364-5367.	0.8	5
128	Abrupt Stress Induced Transformation in Amorphous Carbon Films with a Highly Conductive Transition Phase. Physical Review Letters, 2008, 100, 176101.	2.9	81
129	Monochromatic photoluminescence obtained from embedded ZnO nanodots in an ultrahard diamond-like carbon matrix. Diamond and Related Materials, 2008, 17, 167-170.	1.8	13
130	Fabrication and Characterization of Multilayer Amorphous Carbon Films for Microcantilever Devices. IEEE Sensors Journal, 2008, 8, 616-620.	2.4	5
131	Self-assembled Ni nanoclusters in a diamond-like carbon matrix. International Journal of Nanotechnology, 2007, 4, 424.	0.1	3
132	Mechanical properties of alternating high-low sp3 content thick non-hydrogenated diamond-like amorphous carbon films. Diamond and Related Materials, 2007, 16, 1882-1886.	1.8	24
133	Thermal stability of nonhydrogenated multilayer amorphous carbon prepared by the filtered cathodic vacuum arc technique. Journal of Vacuum Science and Technology A: Vacuum, Surfaces and Films, 2007, 25, 421-424.	0.9	1
134	A Carbon Nanomattress: A New Nanosystem with Intrinsic, Tunable, Damping Properties. Advanced Materials, 2007, 19, 2941-2945.	11.1	44
135	Vibratory response of diamond-like amorphous carbon cantilevers under different temperatures. Diamond and Related Materials, 2004, 13, 1980-1983.	1.8	4